PERGAMON

Available online at www.sciencedirect.com
ScienceDirect

Acta Astronautica 63 (2008) 855–864

ACTA ASTRONAUTICA

www.elsevier.com/locate/actaastro

Radiation dosimetry for high LET particles in low Earth orbit

D. Zhou[a, b, *], D. O'Sullivan[c], E. Semones[a], N. Zapp[a], S. Johnson[a], M. Weyland[a]

[a] *Johnson Space Center, Mailcode SF21, 2101 Nasa Parkway, Houston, TX 77058, USA*
[b] *Universities Space Research Association, 3600 Bay Area Boulevard, Houston, TX 77058, USA*
[c] *Dublin Institute for Advanced Studies, 5 Merrion Square, Dublin 2, Ireland*

Received 9 June 2007; received in revised form 29 February 2008; accepted 9 April 2008
Available online 2 June 2008

Abstract

Research indicates that the impact to human tissues from radiation exposure is strongly related to the LET (linear energy transfer) of the particles and particles with high LET ($\geqslant 5\,\mathrm{KeV}/\mu\mathrm{m}$ water) dominate the damage. High LET radiation in LEO (low Earth orbit) is composed mainly of galactic cosmic rays (GCR), solar energetic particles, particles trapped in the SAA (South Atlantic Anomaly), and albedo neutrons and protons scattered from the Earth's atmosphere. So far the active personal dosimeters are not available and the best passive personal dosimeters currently applied to the radiation assessment for astronauts are CR-39 detectors (for the high LET part) in combination with thermoluminescence detectors (TLDs) or optically stimulated luminescence detectors) (OSLDs) (for the low LET part). LET spectra for radiation in LEO were determined with CR-39. This paper introduces the operational principles for CR-39 detectors, describes the method of LET spectrum using CR-39 and presents the results measured with CR-39 and TEPC (tissue equivalent proportional counter) for space mission ISS-Expedition 2, STS-108, STS-112, ISS-7S, STS-114 and STS-121.
Published by Elsevier Ltd.

Keywords: Space radiation; CR-39 detectors; LET spectrum

1. Introduction

Astronauts are exposed to space radiation which cannot be shielded effectively especially for particles with high linear energy transfer (LET). The radiation of particles in LEO is composed of galactic cosmic rays (GCR), solar energetic particles, particles in the South Atlantic Anomaly (SAA), and albedo neutrons and protons from the Earth's atmosphere. GCR is the main contributor to radiation in LEO. About 98% of particles in GCR are protons and HZE (high energy and high charge) particles. Of these nuclei, 86.5% are protons, 12% are helium ions and about 1.5% are heavier ions. HZE particles, despite their low fluence, make a significant contribution to the radiation dose, because LET is proportional to Z^2. The level of radiation within spacecraft in LEO is determined by altitude, orbital inclination with Earth's equator, spacecraft shielding and the stage of solar activity.

The composition of CR-39 material is $C_{12}H_{18}O_7$, most similar to human tissue and the CR-39 PNTDs (plastic nuclear track detectors) are sensitive to high LET particles. Therefore, CR-39 detectors are most suitable for the simulation and representing the biology

* Corresponding author at: Johnson Space Center, Mailcode SF21, 2101 Nasa Parkway, Houston, TX 77058, USA. Tel.: +1 281 244 6196.

E-mail address: dazhuang.zhou-1@nasa.gov (D. Zhou).

0094-5765/$ - see front matter Published by Elsevier Ltd.
doi:10.1016/j.actaastro.2008.04.002

response of human tissue to radiation with high LET ($\geqslant 5\,\mathrm{keV}/\mu\mathrm{m}$ water).

CR-39 detectors have been playing a unique and important role in the radiation research. The high LET particles measurable with CR-39 detectors include GCR particles, trapped protons in SAA, albedo neutrons and protons, and their charged secondaries (short-range recoils and fragments) produced by the interactions between the primary particles and the nuclei of the CR-39 material. GCR particles are the main radiation contributor among the different types of detectable particles. LET spectra (fluence, absorbed dose and dose equivalent) were measured with CR-39 detectors for the ISS-Expedition 2, STS-108, STS-112, ISS-7S, STS-114 and STS-121.

In addition to the CR-39 detectors, thermoluminescence detectors (TLDs) and optically stimulated luminescence detectors (OSLDs) sensitive to low LET are also widely used for radiation assessment. A combination of passive dosimeters composed of CR-39, TLD or OSLD is suitable for radiation measurement for all LET and can be used as personal dosimeters for astronauts. As the main interest of this paper is high LET radiation, results related to TLD and OSLD are not reported here.

Research has shown that the biological impact of human tissues is strongly related to the LET values of the charged particles. Therefore the measured LET spectra of high LET particles in LEO are of great significance for the insight research of the biological response to the radiation.

This paper introduces the role of high LET particles in radiobiology, the operation principles of CR-39 detectors and the LET spectrum method using CR-39, presents LET spectra and the radiation quantities measured with CR-39 detectors in LEO and compares the results measured with passive CR-39 dosimeters and active dosimeter TEPC.

2. Role of high LET radiation in radiobiology

Research in radiobiology indicates that high LET radiation is much more effective than low LET radiation in the induction of biological effects and the RBE (relative biological effectiveness) for chromosomal, cellular and tissue increases with LET [1–6]. Fig. 1 shows the relationship of cross section of tumor induction and LET, and Fig. 2 shows the relationship of tumor prevalence and particles' fluence and LET. The two figures show that both the living tissue damage and tumor risk strongly depends on the particle's LET, and high LET radiation is dominant for the biological impact. Therefore radiation measurement and research for high LET particles should be emphasized and the systematic measurements for space radiation with high LET should be conducted, especially using the dosimeters available now for astronauts.

The possibility of the tumor prevalence induced by high LET radiation can be estimated if the LET spectrum of radiation with high LET in space is measured systematically. The investigation combining the radiobiology research and the radiation measurement in space is needed and is one of our long term tasks for the research of space radiation.

3. CR-39 detectors for radiation measurement

3.1. Operation principles of CR-39 detectors

CR-39 detector is light weight, small volume, electronics free, easy to process and very cheap comparing to any active dosimeters. All the CR-39 materials used by JSC (Johnson Space Center) and DIAS (Dublin Institute for Advanced Studies) researchers were manufactured by American Technical Plastics. The threshold of LET for the material is $\sim 5\,\mathrm{keV}/\mu\mathrm{m}$ water.

When charged particles pass through CR-39 detector, they lose energy through ionization and break the molecular bonds of the CR-39 polymer to form high reactive paths along their trajectories. These paths can be revealed as the etched cones on the surfaces of the CR-39 detectors by chemical etch and the etched cones can be observed with microscope.

CR-39 detectors are sensitive to high LET radiation and can measure the LET spectrum (differential and integral fluence, absorbed dose and dose equivalent) for charged particles with high LET directly. CR-39 can also measure radiation for high energy protons and neutrons through their secondary charged particles (short-range high LET recoils and target fragments).

The tracks observed on the surfaces of CR-39 detector were due to short range recoils and fragments coming from the nuclear interactions of protons, neutrons and heavy nuclei in the CR-39 detectors as well as the trajectory tracks due to the passage of the long range primary cosmic rays and secondary HZE particles. The two types of events with different ranges can be easily separated experimentally since the tracks produced by short range recoils and fragments can only be observed on one surface of CR-39 detectors while tracks produced by long range HZE particles can be observed on at least two surfaces or in more than two sheets of CR-39 as coincident etched cones.

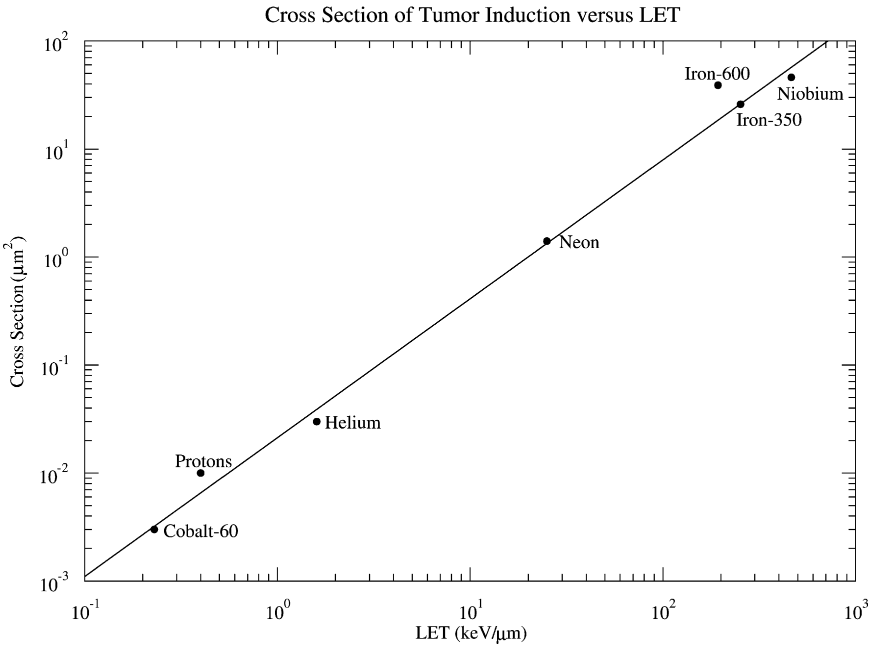

Fig. 1. Cross section (the risk coefficient) as a function of LET [1].

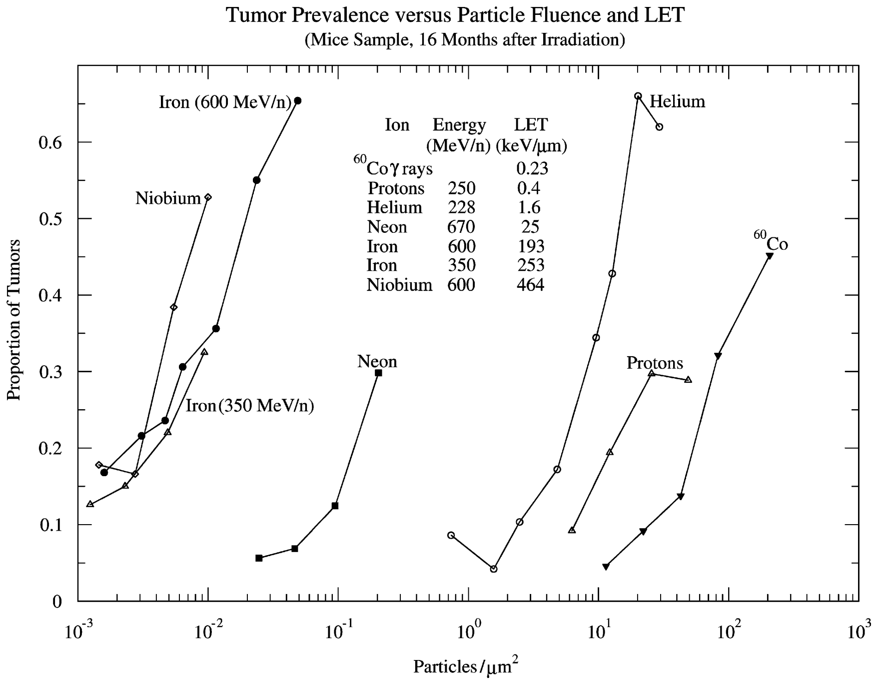

Fig. 2. Tumor prevalence as a function of particle fluence and LET [1].

Therefore CR-39 detectors can measure total dose and dose equivalent which is contributed by all kinds of particles (primary and secondary particles including HZE particles) and that contributed by HZE particles only.

3.2. Two different approaches to detect charged particles

The charged particles can be measured by either the coincidence approach for long range HZE particles

Table 1
The energy intervals of nuclei detectable by CR-39 detectors as coincidence events

Nuclei	Charge	Energy interval detectable by CR-39 (MeV/n)
		E_1–E_2
H	1	7.5–10
He	2	8–50
Li	3	9–150
B	5	12–1200
C	6	$14\leqslant$
N	7	$15\leqslant$
O	8	$16\leqslant$
Ne	10	$18\leqslant$
Mg	12	$20\leqslant$
Si	14	$22\leqslant$
Fe	26	$28\leqslant$

(mainly GCR heavy nuclei) or non-coincident approach for low energy and short range particles (mainly secondary recoils and fragments).

The concept of energy intervals detectable for charged particles in CR-39 is important to understand the physical principles of the methods for radiation measurement using CR-39 detectors. The energy intervals of charged particles detectable by CR-39 detectors as coincident events are listed in Table 1. In the calculation, a minimum LET of ~5 keV/μm water was used to determine the maximum energy. To determine the minimum energy of particles, we assumed that at least one plate of CR-39 with a thickness of ~600 μm was traversed by particles.

The detection approaches for charged particles with CR-39 detectors can be described briefly below. Particles with energies within the energy interval can be detected directly as coincidence events, because the nuclear tracks are formed in both surfaces of CR-39 detector. Particles with energies lower than E_1 can be detected directly also, but as higher LET events and the nuclear tracks are formed in one surface of CR-39 detector only. Particles with $Z\leqslant 5$ and energies higher than E_2 can be detected as short-range, high LET secondaries (recoils and fragments). Therefore, all particles (primary and secondary) can be measured by the nuclear tracks in one surface of CR-39 detector and HZE particles can be measured as coincidence events.

The method to find out long range HZEs can be described as below. In the procedure of data scan on the top surface of the CR-39 detector, every selected etched cone is focused downwards to the bottom surface along the direction of major axis for the top cone to determine the event is coincident or not, if a symmetric bottom cone is found, the event is coincident and the particle is selected as long range HZE particle. Research indicates that the majority of HZE particles measured by this approach are primary GCR heavy ions.

Therefore, CR-39 dosimeters can measure radiation directly or through secondaries for both charged particles and neutrons and are very useful for the radiation measurement and research.

4. LET spectrum method for radiation measurement using CR-39 PNTDs

4.1. Radiation exposure of CR-39 detectors and chemical etch of detectors

In our experiments of radiation exposure in LEO, CR-39 detectors were either carried by astronauts or located in the selected monitoring areas inside the spacecraft or attached to the active dosimeter JSC-TEPC with an LET threshold of 0.2 keV/μm water. Radiation measurement was conducted for space mission ISS-Expedition 2 (April–August 2001), STS-108 (December 2001), STS-112 (October 2002), ISS-7S (October 2003), STS-114 (July–August 2005) and STS-121 (July 2006).

After exposure and recovery, the plates of CR-39 were chemically etched (NaOH, 6.25 N, 60 °C). In the procedure of etching, the chemical solution attacks the surface of the CR-39 sheet and dissolves it at a constant etch rate. There is a preferential or faster etch along the direction of particle's trajectory where the polymer has been damaged by the energy deposit from charged particles. The results of the chemical etch will form etched cones on the surface of CR-39 detector which can be observed with a microscope.

After etch, the thickness and the mass before and after etch for the CR-39 plate are measured and the bulk etch B—the thickness etched off on one surface of the CR-39 detector—was calculated by Henke's formula [7]:

$$B=\frac{(m_1-m_2)T_2}{2m_2}\left(1-\frac{pT_2}{2A_d}\right)$$

where m_1 is the detector mass before etch, m_2, the mass after etch; T_2, the average detector thickness after etch; p, the detector perimeter and A_d, the detector surface area. Bulk etch rate V_B is then calculated by $V_B=B/t$, where t is the etch time. The bulk etch formula indicates that the variation of bulk etch is small if the variation of CR-39 thickness is small.

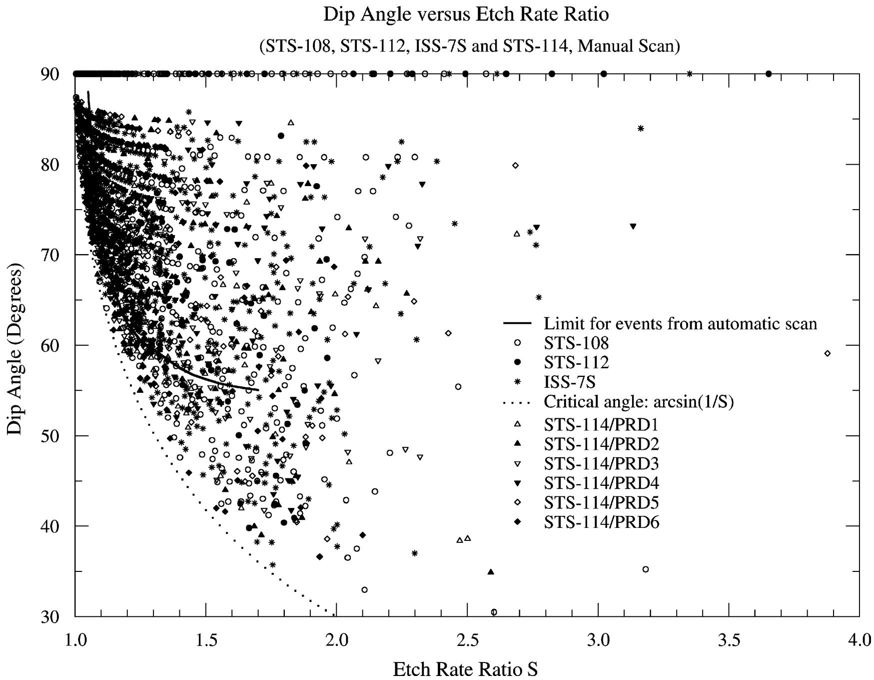

Fig. 3. Comparison of manual scan and automatic scan for STS and ISS missions.

4.2. Data acquisition by manual scan

Research indicates that the surface area of the etched cone is a function of the LET for the incident charged particle [8–10,18], thus data collection for CR-39 detectors can be simplified to the collection of the major and minor axes for the cone surface.

Following etch, events were identified and the major and minor axes of the etched track cones on the CR-39 surface were measured and collected with optical microscope with either manual scan or semi-automatic scan (events viewed and adjusted by human eyes).

A difficult aspect for LET spectrum work using CR-39 detectors and microscope is to distinguish and collect real events which represent particle radiation from other sources. There are two kinds of etched cones, one represents real events and the other represents non-real spots resulting from material defects of CR-39. In some cases the non-real spots are even dominated. Computer automatic scan tends to collect more non-real spots and will also incorrectly read and collect some real events with big dip angle and events overlapped each other, no matter how the software is adjusted. Another difficulty for automatic scanning occurs when the spots resulting from material defects of CR-39 are highly un-isotropically distributed, even for the different areas in the same plate of CR-39. Therefore, if many such spots are collected as real events from either flown CR-39 or ground control CR-39, the net radiation quantities (background subtracted) will be far from the real ones. These two problems will make the scanned data less-reliable if the fully-automatic scan is used without human eye's modification. The experienced researchers can distinguish real events from non-real ones and judge the events with big dip angle correctly, increasing the reliability of scanned data.

Another big advantage of manual scan is to recognize and collect data for HZE particles in the same procedure of normal scan and for the same scanned area.

As to the scan speed, for an experienced researcher the manual scan is usually several times faster than the semi-automatic scan, because the conductor of semi-automatic scan must spend much time to removing the non-real or bad events from the computer-selected events roster, and/or to adjust the major and minor axes many times for the same event.

Due to the unique advantages of manual scan, the data scan and collection for CR-39 detectors was conducted manually at JSC-SRAG and DIAS.

Fig. 3 shows a comparison for the data scanned with manual scan and automatic scan for some STS and ISS missions. In the figure the dip angle is $\geqslant 55°$ and the etch rate ratio S (see section below for the definition) is $\leqslant 1.7$ for most events from automatic scan [11] while

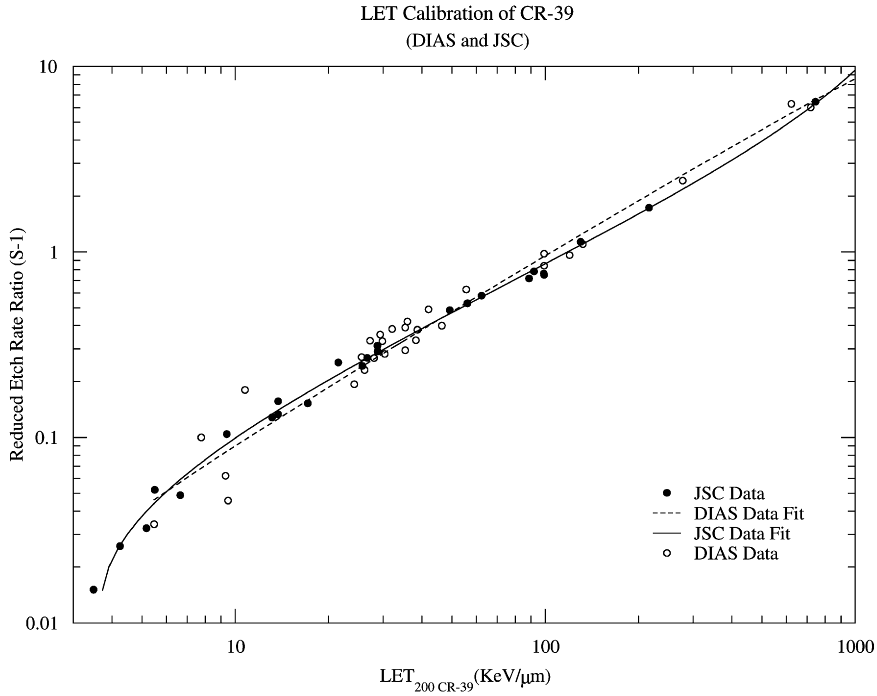

Fig. 4. LET calibration for CR-39 detectors.

the dip angle is as low as to 30° and the etch rate ratio is as high as ~4 for events from manual scan [12–14]. The figure indicates that the scanning efficiency of the manual scan is higher.

4.3. LET calibration for CR-39 detectors

Physical quantities LET_{200} CR-39 and etch rate ratio are used to express the LET calibration of CR-39 detectors. The LET_{200} CR-39 is defined as the restricted energy loss in CR-39 which produces delta rays with energies less than 200 eV and, the etch rate ratio is defined as $S = V_T/V_B$, where V_T is the track etch rate defined as $V_T = L_0/t$, where L_0 is the length from pre-etch surface to the etched cone tip measured along the particle's trajectory and t is the etch time.

The relationship between LET_{200} in CR-39 and etch rate ratio S was determined by calibrating the CR-39 detectors with heavy ions and protons. Accelerator centers Darmstadt, HIMAC, NSRL, BNL and the Cyclotron Institute at Texas A and M University (TAMU) can provide a variety of heavy ions and protons. The DIAS LET calibration [12,13] was used for the STS-108, STS-112 and ISS-7S flights, the updated Benton calibration [15] obtained by JSC was used for ISS-Expedition 2, and the JSC calibration [14,16,24] was used for STS-114 and STS-121.

The LET_{200} CR-39 values of the charged particles can be calculated either by computer codes or Benton table [17] and, the etch rate ratio can be calculated with Somogyi's formula [18]:

$$S = \sqrt{1 + 4\left(\frac{a}{2B}\right)^2 \Big/ \left[1 - \left(\frac{b}{2B}\right)^2\right]^2}$$

where a and b are the major and minor axes, respectively. A homogenous bulk etch rate throughout the detector surface is a necessary and essential condition to hold the formula, and more intensive study for the impact of the variation in B engendered by the inhomogenous bulk etch rate is needed.

Thus the relationship between LET_{200} CR-39 and etch rate ratio S is obtained. Fig. 4 shows the LET calibrations for CR-39 detectors conducted by different institutes and used for different space missions.

4.4. LET spectrum generating

The LET values of the scanned events can be calculated using LET calibration for CR-39 detectors once the etch rate ratio is known. The LET spectra can then be generated and the radiation quantities can be obtained based on the LET spectrum method using CR-39 detectors [12–14,16,19–22] which is described in detail as below.

Research indicates that the radiation field in LEO is nearly distributed isotropically. For the isotropically distributed radiation field, the differential fluence F is described by

$$F = (2\pi A \cos^2 \delta_{\mathrm{cut}})^{-1} \frac{\mathrm{d}N}{\mathrm{dLET}}$$

where F is the differential fluence in particles/(cm^2 sr keV/μm water); A, the scanned detector area; dLET, the LET bin; dN, the number of events in dLET; δ_{cut}, the cutoff angle of the dip angle (particle's incident angle to the detector), above which the detection efficiency of CR-39 detector is 100% [19,20].

The net differential fluence is obtained by subtracting the ground background radiation from the total differential fluence, which is contributed by both space and background radiation.

The differential absorbed dose in Gy is then

$$4\pi \times 1.6 \times 10^{-9} \times \mathrm{LET}_{\infty} \times F$$

where LET_{∞} is the linear energy transfer in keV/μm water. The differential dose equivalent is obtained as Dose$\times Q$, where Q is the quality factor recommended by ICRP-60.

The integral spectrum is generated by summing the differential spectrum from high LET to low LET. Thus the absorbed dose and dose equivalent ($\geqslant$LET) can be obtained from the integral spectra of absorbed dose and dose equivalent.

The average quality factor $Q_{\mathrm{ave.}}$ ($\geqslant$LET) is calculated by

$$Q_{\mathrm{ave}}(\geqslant \mathrm{LET}) = \text{integral dose equivalent } (\geqslant \mathrm{LET}) \\ /\text{integral absorbed dose}(\geqslant \mathrm{LET})$$

The relationship of LET_{∞} in water and LET_{200} in CR-39 can be expressed as [12]

$$\log(\mathrm{LET}_{\infty}\mathrm{water}) = 0.1689 + 0.984 \log(\mathrm{LET}_{200}\mathrm{CR\text{-}39})$$

The formula indicates that the conversion factor varies from 1.32 at ∼1000 keV/μm CR-39 to 1.44 at ∼5 keV/μm CR-39.

5. LET spectra of high LET particles measured in LEO

Fig. 5 shows the integral spectra of dose equivalent and Fig. 6 shows the average quality factors determined with CR-39 detectors for the ISS-Expedition 2, STS-108, STS-112, ISS-7S, STS-114 and STS-121 missions [12–14,16,20–23]. In the two figures and in Table 2

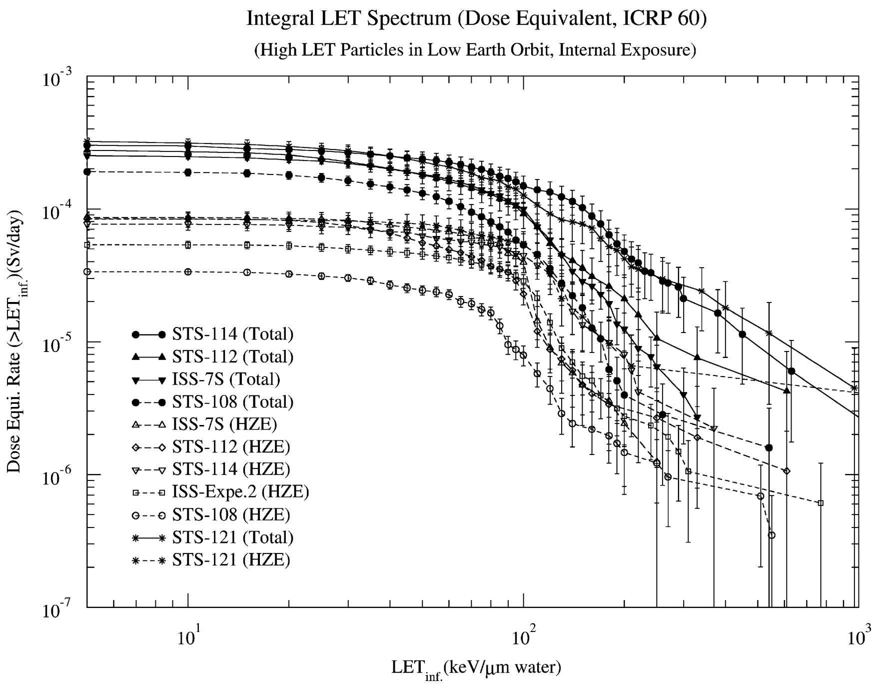

Fig. 5. Integral LET spectra of dose equivalent for high LET particles in LEO.

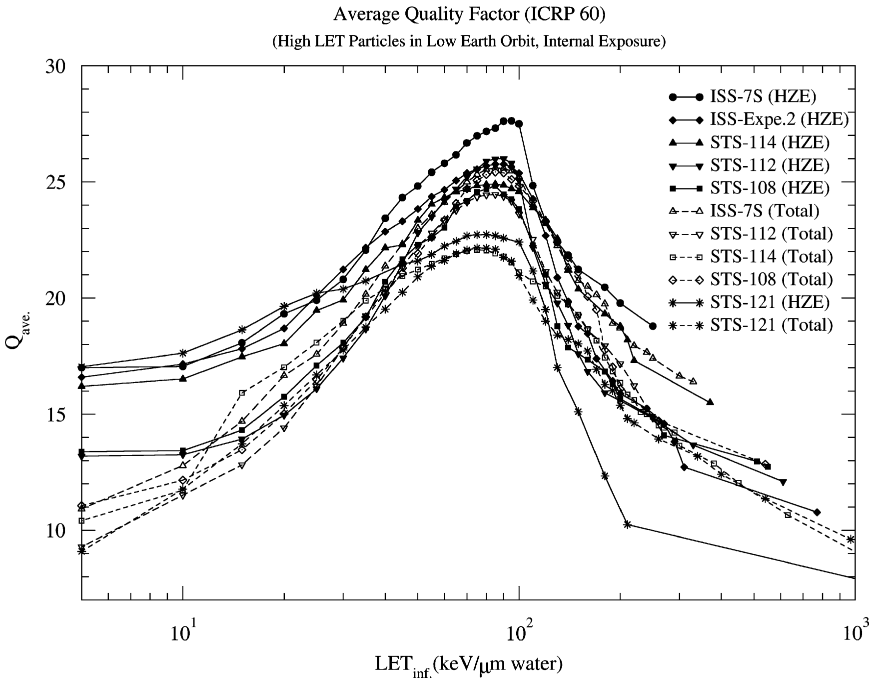

Fig. 6. The average quality factors for high LET particles in LEO.

Table 2
Absorbed dose and dose equivalent measured with CR-39 PNTDs and TEPC in LEO (inclination: 51.6°; inside exposure: $\geqslant 10$ KeV/μm water)

Mission	Particles	Absorbed dose rate (μGy/day)	Dose equi. rate (ICRP 60) (μSv/day)	Quality factor
ISS-Expedition 2 (April–August 2001)	CR-39 (Total)	25.99 ± 1.94	297.66 ± 22.19	11.45
	CR-39 (HZE)	3.12 ± 0.19	53.56 ± 3.28	17.15
STS-108 (December 2001)	CR-39 (Total)	15.48 ± 0.75	188.25 ± 11.33	12.16
	CR-39 (HZE)	2.50 ± 0.12	33.59 ± 1.57	13.43
STS-112 (October 2002)	TEPC (Total)	24.76 ± 0.47	268.07 ± 5.06	10.83
	CR-39 (Total)	23.65 ± 1.67	277.73 ± 19.64	11.74
	CR-39 (HZE)	6.33 ± 0.32	83.96 ± 4.18	13.26
ISS-7S (October 2003)	CR-39 (Total)	19.36 ± 0.71	247.57 ± 9.13	12.79
	CR-39 (HZE)	4.85 ± 0.36	82.72 ± 6.13	17.05
STS-114 (July-August 2005)	TEPC (Total)	25.52 ± 0.65	285.13 ± 7.24	11.17
	CR-39 (Total)	25.36 ± 1.62	297.53 ± 19.05	11.73
	CR-39 (HZE)	4.64 ± 0.46	76.63 ± 7.51	16.51
STS-121 (July 2006)	TEPC (Total)	26.89 ± 0.69	300.01 ± 7.70	11.16
	CR-39 (Total)	26.60 ± 1.86	313.04 ± 22.19	11.77
	CR-39 (HZE)	4.74 ± 0.63	83.56 ± 11.07	17.62

below, 'total' means all types of primary and secondary particles including HZE particles. The quality factors of high LET radiation for both all particles and HZE particles are from $\sim > 12$ at ~ 10 keV/μm water to $\sim > 22$ at ~ 85 keV/μm water.

Table 2 is a collection for the absorbed dose and dose equivalent measured with CR-39 detectors for some space missions in LEO since 2001. Radiation measured with TEPC contributed by all particles is also collected in the table. Radiation measured by CR-39 is mainly

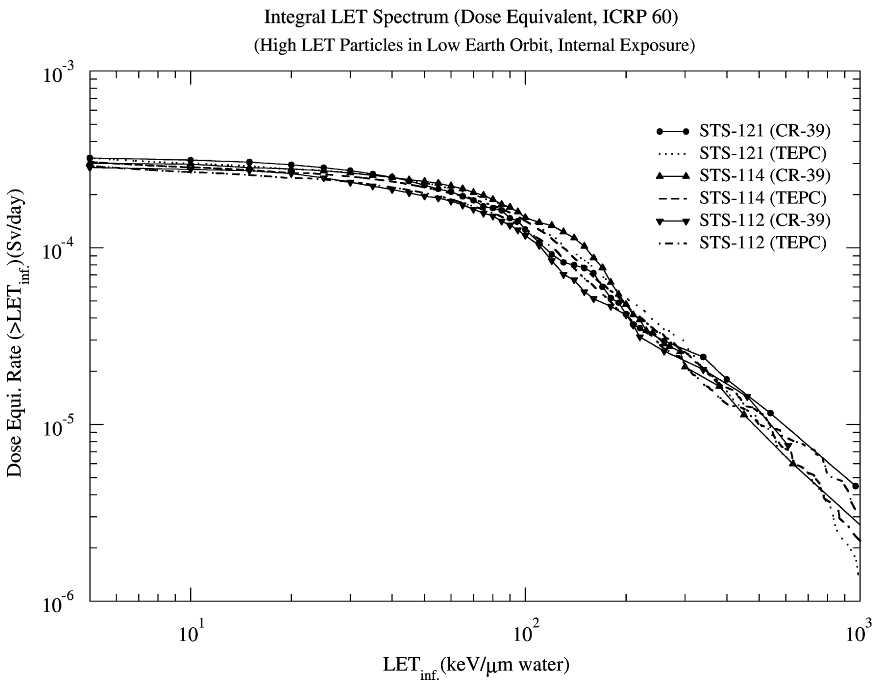

Fig. 7. Comparison of dose equivalent measured with CR-39 detectors and TEPC.

contributed by the short range recoils and fragments (secondary particles of primary charged particles and neutrons) and long range HZE particles. The comparisons for the values of the absorbed dose and dose equivalent measured with active dosimeters TEPC and passive CR-39 dosimeters show excellent agreement.

Fig. 7 shows the comparison of the integral spectra of dose equivalent (ICRP 60) measured with CR-39 PNTDs and TEPC for STS-112, STS-114 and STS-121 space missions. In addition to Table 2, Fig. 7 also shows that the dose equivalent for the radiation field with high LET in low Earth orbit measured with different active and passive dosimeters agrees very well.

Estimation of tumor risk for human from the exposure of high-LET particles in LEO can then be carried out principally based on the experimental data showed in Figs. 2 and 5. However, this topic is beyond the scope of this paper and cannot be discussed here in detail.

6. Conclusions

Particles with high-LET in LEO play a dominant role for the radiation impact on astronauts; CR-39 detectors are most suitable for the measurement of high-LET particles and the LET spectrum method using CR-39 detectors is important and reliable. Systematic measurements of the absorbed dose and dose equivalent were obtained with CR-39 detectors for recent space missions. These experimental results are unique and useful for the estimation of the tumor risk for human from high LET exposure. Further investigation should be conducted for radiation research related to the high LET particles.

Acknowledgments

The authors sincerely thank all those who assisted them in their work at Darmstadt, CERN, HIMAC, TAMU, BNL and on ISS-Expedition 2, STS-108, STS-112, ISS-7S, STS-114 and STS-121 space missions.

References

[1] E.L. Alpen, S.B. Powers-Risius, S.B. Curtis, R. Deguzman, Tumorigenic potential of high-*Z*, high-LET charged-particle radiations, Radiation Research 136 (1993) 382–391.

[2] NCRP, Radiation protection guidance for activities in low-Earth orbit, NCRP Report 132, 2000.

[3] NCRP, Operational radiation safety program for astronauts in low-Earth orbit: a basic framework, NCRP Report 142, 2002.

[4] H. Wu, K. George, V. Willingham, T. Kawata, F.A. Cucinotta, Comparison of *F* ratios generated from interphase and metaphase chromosome damage induced by high doses of low- and high-LET radiation, Radiation Research 155 (2001) 57–62.

[5] F.A. Cucinotta, M.H.Y. Kim, L. Ren, Managing lunar and Mars mission radiation risks Part I: cancer risks, uncertainties and shielding effectiveness, JSC-NASA Internal Report, May 2005.

[6] M. Hada, F.A. Cucinotta, S.R. Gonda, H. Wu, mBAND analysis of chromosomal aberration in human epithelial cells exposed to low- and high-LET radiation, Radiation Research 168 (2007) 98–105.
[7] R.H. Henke, K. Ogura, E.V. Benton, Standard method for measurement of bulk etch in CR-39, Nuclear Tracks 12 (1986) 307–310.
[8] R. Fleischer, P.B. Price, R.M. Walker, Nuclear Tracks in Solids, University of California Press, Berkeley, CA, 1975.
[9] G. Giacomelli, L. Patrizii, V. Popa, P. Serra, V. Togo, New results from exposures of CR-39 nuclear track detectors, Radiation Measurements 28 (1997) 217–222.
[10] S. Balestra, M. Cozzi, G. Giacomelli, et al., Bulk etch rate measurements and calibrations of plastic nuclear track detectors, Nuclear Instruments and Methods B 254 (2007) 254–258.
[11] R. Keegan, LET spectrum generation and ^{1}H induced secondary contribution to total dose measured in low Earth orbit, Ph.D. Thesis, Department of Experimental Physics, University College Dublin, National University of Ireland, 1996.
[12] D. O'Sullivan, D. Zhou, E. Semones, et al., Dose equivalent, absorbed dose and charge spectrum investigation in low Earth orbit, Advances in Space Research 34 (2004) 1420–1423.
[13] D. Zhou, D. O'Sullivan, E. Semones, et al., Dose equivalent, absorbed dose and charge spectrum measurements made in the international space station orbit, in: Proceedings of 28th International Cosmic Ray Conference, 2003, pp. 2263–2266.
[14] D. Zhou, D. O'Sullivan, E. Semones, M. Weyland, Charge spectra of cosmic ray nuclei measured with CR-39 detectors in low Earth orbit, Nuclear Instruments and Methods A 564 (2006) 262–266.
[15] E.R. Benton, Radiation dosimetry at aviation altitudes and in low-Earth orbit, Ph.D. Thesis, Department of Experimental Physics, University of College Dublin, National University of Ireland, 2004.
[16] D. Zhou, E. Semones, M. Weyland, S. Johnson, Radiation measured with TEPC and CR-39 PNTDs in low Earth orbit, Advances in Space Research 40 (2007) 1571–1574.
[17] E.V. Benton, R.P. Henke, Heavy particle range–energy relations for dielectric nuclear track detectors, Nuclear Instruments and Methods 67 (1969) 87–92.
[18] G. Somogyi, Processing of plastic track detectors, Nucl. Track Detectors 1 (1977) 3–18.
[19] D. O'Sullivan, D. Zhou, W. Heinrich, et al., Cosmic rays and dosimetry at aviation altitudes, Radiation Measurement 31 (1999) 579–584.
[20] D. Zhou, Radiation of cosmic rays and dosimetry at aviation altitudes, Ph.D. Thesis, Departmental of Experimental Physics, University College Dublin, National University of Ireland, 1999.
[21] D. Zhou, D. O'Sullivan, E. Semones, et al., Radiation field of cosmic rays measured in low earth orbit, by CR-39 detectors, Advances in Space Research 37 (2006) 1764–1769.
[22] D. Zhou, E. Semones, R. Gaza, M. Weyland, Radiation measured with passive dosimeters in low Earth orbit, Advances in Space Research 40 (2007) 1575–1579.
[23] D. Zhou, E. Semones, R. Gaza, S. Johnson, N. Zapp, M. Weyland, Radiation measured for ISS-Expedition 12 with different dosimeters, Nuclear Instruments and Methods A 580 (2007) 1283–1289.
[24] D. Zhou, E. Semones, M. Weyland, E.R. Benton, LET calibrations for CR-39 detectors in different oxygen environment, Radiation Measurement 42 (2007) 1499–1506.